

From Ar Clustering Dynamics to Ar Solvation for Na⁺–Benzene

M. Albertí,* A. Aguilar, and J. M. Lucas

Departament de Química Física i Centre de Recerca en Química Teòrica, Parc Científic, Universitat de Barcelona. Martí i Franquès, 1, 08028 Barcelona, Spain

A. Laganà and F. Pirani

Dipartimento di Chimica, Università di Perugia, 06123 Perugia, Italy

Received: October 23, 2006; In Final Form: November 30, 2006

The gradual evolution from cluster rearrangement to solvation dynamics is discussed by considering the rearrangement of n ($n = 1, \dots, 19$) Ar atoms around Na⁺–benzene clusters and using an atom–bond potential energy surface. The nature of the bonding is discussed on the basis of the decomposition of the interaction energy and of the formation of the possible conformers. The benzene molecule is found to remain strongly bound to Na⁺ independently of the number of solvating rare-gas atoms, although due to the anisotropy of the interaction potential, the Ar atoms solvate the Na⁺–benzene cluster preferentially on the side of the cation. Other specific features of the solvation process are discussed.

1. Introduction

In recent years, significant progress has been made in generating van der Waals clusters consisting of a molecule embedded in a flexible cage of surrounding molecules.¹ These experimental advances have fostered theoretical studies on the structure and dynamics of clusters. This is the case of large neutral van der Waals complexes, as those formed by aromatic molecules surrounded by rare-gas (Rg) atoms. The study of these clusters, generated either via supersonic expansion or gas condensation, provides more general structural and energetic information on the solvation mechanisms thanks to the fact that inert gas atoms are believed to be a suitable prototype for modeling solvents.² Aromatic molecule–rare gas complexes can be, in fact, viewed as a solute molecule caged in a well-characterized local solvent configuration,³ and the solvation mechanisms can be related to both the existence of different minima in the potential energy surface (PES)⁴ and the modification of the various layers⁵ of solvent. The same approach can be adopted for ionic clusters once the components of the interaction have been properly represented.^{6–9}

The proper representation of the interaction components and the consequent molecular dynamics study of the solvation processes on the resulting force field has been the focus of most of our recent research efforts.^{10–15} In particular, we have considered the clusters formed by benzene (bz),¹¹ K⁺–bz,¹² Cl[–]–bz,¹³ and Rb⁺–bz¹⁵ with a few Ar atoms. These studies have singled out the importance of choosing appropriate formulations for the components of the force field, making them suitable to describe the stabilization effect of the ion, the mechanism through which the rare gas atoms tend to condense on the same side of the benzene plane and the role played by the size of the ion on clusterization mechanisms. Taking into account that size specific interaction of alkali metal ions with aromatic side chains has been proposed as a mechanism for selectivity in some K⁺ channel proteins;⁸ the study of systems containing aromatic compounds such as benzene interacting with alkali ions can be very useful to model biological channels.

This paper deals with the extension of the cation series to Na⁺ and with the increase of the number of Ar atoms beyond that of the first solvation layer. Accordingly, the paper is articulated as follows: In Section 2, the construction of the PES, the characterization of most stable isomers, and the description of the isomerization processes are reported. In Section 3, the solvation processes for the single Na⁺ cation, the single benzene molecule, and the benzene–cation aggregate are analyzed in detail.

2. Potential Energy Surface Features and Isomeric Transformations of the Na⁺–Benzene–Ar_{*n*} Clusters

The potential energy functions most often used to describe clusters bound by noncovalent forces express the total interaction as a pairwise summation of atom–atom model potentials.¹⁶ This is based on the fact that these interactions are dominated by pairwise additive two-body forces.² However, in the literature, the need for including contributions other than the pure two atom ones has been repeatedly discussed, with specific focus on microsolvation of both benzene^{5,17–19} and Na⁺ by rare-gas atoms.^{20,21} To better represent these contributions without losing the advantage of formulating the interaction as a sum of two-body-like terms, we have developed an alternative representation of the force field based on atom (ion) molecular bond functionals, which, in spite of their seemingly two-body form, incorporate some many-body effects.

2.1. The Formulation of the Atom–Bond Potential. As already mentioned, the alternative functional representation of the atom (ion)–molecule interaction adopted by us is of the atom (ion)–bond type. Such a functional representation has been described in detail in refs 12–14, where it has been shown how to incorporate the ion molecular quadrupole effect for ion–benzene systems. Accordingly, the total potential energy, V_{total} , is expressed as the sum of an electrostatic (V_{el}) and a nonelectrostatic (V_{nel}) term. For the system considered here, the V_{el} term is made only of the ion–molecular quadrupole contribution. This means that it is formulated as a sum of the Coulombic interactions associated with the cation, the negative charges

* Corresponding author. E-mail: m.alberti@ub.edu.

placed both above and below (with respect to the molecular plane) the C atoms and the positive charges placed at the center of the H atoms of benzene. V_{el} has already been found to play a key role in differentiating the properties of the cation–bz heteroclusters¹² from those of the anion–bz ones.¹³

V_{nel} is formulated as a combination of a repulsion and an attraction term in which dispersion and induction attractions, dominant at long range, are counterbalanced by exchange (size) repulsion effects, prevalent at short range. In our case, to describe cation–bz systems, V_{nel} is made of 12 ion–bond terms^{12,13} having the form

$$V(r, \alpha) = \epsilon(\alpha) \left[\frac{m}{n(r, \alpha) - m} \left(\frac{r_0(\alpha)}{r} \right)^{n(r, \alpha)} - \frac{n(r, \alpha)}{n(r, \alpha) - m} \left(\frac{r_0(\alpha)}{r} \right)^m \right] \quad (1)$$

It is important to emphasize here that r is the distance of the atom (or the ion) from the center of the considered bond (and not the internuclear distance) and α is the angle that the bond and r form. The parameter m is taken equal to 6 for atom–bond interactions and 4 for ion–bond ones. The parameters ϵ and r_0 , representing respectively the depth of the potential well and the location of the well minimum, are expressed as a functions of α in terms of their parallel (ϵ_{\parallel} and $r_{0\parallel}$) and perpendicular (ϵ_{\perp} and $r_{0\perp}$) values using simple trigonometric formulas.^{12,13} Quoted values of ϵ and r_0 are derived from the charge and the polarizability of the related atomic species as well as polarizability and effective polarizability tensor components of aromatic CC and CH bonds. The parameter n is then expressed as a function of both r_0 and r ,¹⁰

$$n(r, \alpha) = \beta + 4.0 \left(\frac{r}{r_m(\alpha)} \right)^2 \quad (2)$$

with the β parameter being set, in our case, equal to 10.0. The nonelectrostatic interaction of Ar and Na⁺ with benzene is then given as a sum of 12 atom (ion)–bond terms of the type shown in eq 1. The corresponding values of the parameters for the Rg–bz and cation–bz systems are taken from refs 10 and 14. The interactions Na⁺–Ar and Ar–Ar are formulated as in eq 1 once the angular dependence is removed. Related parameters are taken from refs 22 and 23.

Accordingly, For Na⁺–benzene–Ar_{*n*} clusters, V_{nel} has the following form

$$V_{\text{nel}} = \sum_{i=1}^6 (V_{\text{Na}^+-(\text{CC})_i} + V_{\text{Na}^+-(\text{CH})_i}) + \sum_{j=1}^n \sum_{i=1}^6 (V_{\text{Ar}_j-(\text{CC})_i} + V_{\text{Ar}_j-(\text{CH})_i}) + \sum_{j=1}^n V_{\text{Na}^+-\text{Ar}_j} + \sum_{j=1}^{n-1} \sum_{k=j+1}^n V_{\text{Ar}_j-\text{Ar}_k}$$

while V_{el} , calculated as explained before, is expressed as

$$V_{\text{el}} = \sum_{i=1}^{18} \frac{q_{\text{Na}^+} q_i}{4\pi\epsilon_0 r_{\text{Na}^+-q_i}}$$

where the sum is over 18 charges, 6 of +0.092 45 on each H atom and 12 negative charges of –0.046 23 placed on the C atoms of benzene on both sides of aromatic ring.

This formulation of the total interaction potential accounts for nonadditive effects via a controlled decrease of the polarizability values with respect to their values in isolated molecules.¹²

2.2. The Stable Configurations of the Na⁺–Benzene–Ar_{*n*} Clusters. The large number of degrees of freedom of this type of clusters leads, as an obvious consequence, to quite structured PESs. This means that there are various configurations of these clusters that are stabilized by a corresponding well on the PES. In particular, the single Ar cluster, Na⁺–bz–Ar, forms two quite stable geometries. The most stable of these has the Ar atom placed on the same side of the aromatic ring as the cation. The preference of the Ar atoms to sit on the same side of Na⁺ persists when their number increases. Accordingly, also the number of different spatial arrangements of the Na⁺–bz–Ar_{*n*}, having similar stabilization energies, increases. To identify those having similar stabilization energies, the notation (1 + *n*₁|*n*₂) was adopted. In this notation, figure 1 refers to the ion, while the following indices *n*₁ and *n*₂ refer to the number of Ar atoms placed, respectively, on the same side and on the opposite side of the aromatic ring with respect to the cation (please note that hereafter *n* (*n* = *n*₁ + *n*₂) is used to indicate the total number of Ar atoms). We also use the notations (*n*₁|*k*|*n*₂) and (1+*n*₁|*k*|*n*₂) when *k* of the *n* Ar atoms are placed on (or very close to) the benzene plane.²⁴

The contribution to total energy given by the configuration energy of a particular cluster arrangement has been evaluated using dynamical simulations. The dynamics of the various clusters has been studied by investigating the behavior of microcanonical ensemble (*NVE*) of atoms and treating the benzene molecule as a rigid body. Several molecular simulations have been carried out at different total energy, E_{total} , values using the DL_POLY suite of codes.²⁵ During the simulation, the interaction energy was calculated at every integration step for all atom–bond and atom–atom pairs without imposing any cutoff radius. A time step of 1 fs was used for the integration of the dynamics equations. This allowed us to keep the relative rms fluctuations of E_{total} as small as 10^{–5}. The simulation time was set at 25 ns, a duration long enough to ensure that the mean values of the various energy contributions and the temperature, T , do not further change when extending the calculations to longer times.

In particular, from dynamical calculations, the equilibrium configuration energy, E_{cfg} , (the minimum potential energy), the potential energy value averaged over all accessible configurations at the chosen T value was calculated. These dynamical simulations were repeated for various very low temperatures (below 15 K) and the results were extrapolated to $T = 0$ K. This means that the resulting (extrapolated) value of E_{cfg} tends to coincide with the minimum of the potential energy (V_{total}). An increase of the number of Ar atoms makes the number of accessible configurations quite large. This implies that it becomes increasingly more difficult to appreciate the variation of the relevant energetic contributions and to assign a specific geometry to a given E_{cfg} value even at fairly low temperature. For illustrative purposes, we give in Table 1 the limiting value of E_{cfg} ($T \rightarrow 0$) of the most stable configuration of the (1 + *n*|0) type when *n* varies from 1 to 14. In the table are also given some of the E_{cfg} key components (like $E_{\text{Na}^+-\text{bz}}$, including the electrostatic and the nonelectrostatic contributions and $E_{\text{bz}-\text{Ar}}$ and the bond energy (E_{bond}) that is made of all the pair interactions).

As shown by the Table, the interaction between benzene and Na⁺ is strong and the corresponding energy is only slightly modified when the number of surrounding Ar atoms becomes larger than 6. Moreover, $E_{\text{bz}-\text{Ar}}$ decreases with the number of solvent atoms up to *n* = 9. Then, for 9 ≤ *n* ≤ 14, it stays nearly constant. These results suggest that, at *n* = 8, a kind of complete

TABLE 1: Energy of the Different Isomers for the $\text{Na}^+ - \text{bz} - \text{Ar}_n$ Clusters ($n = 1, \dots, 14$)

n	$E_{\text{cfg}}/\text{meV}$	$E_{\text{Na}^+ - \text{bz}}/\text{meV}$	$E_{\text{bz} - \text{Ar}}/\text{meV}$	$E_{\text{bnd}}/\text{meV}$	isomer
1	-1446	-1249	-32	-167	(1 + 1 0)
2	-1656	-1249	-63	-346	(1 + 2 0)
3	-1869	-1249	-93	-529	(1 + 3 0)
4	-2086	-1249	-120	-717	(1 + 4 0)
5	-2159	-1249	-143	-767	(1 + 5 0)
6	-2233	-1249	-168	-816	(1 + 6 0)
7	-2399	-1246	-155	-998	(1 + 7 0)
8	-2463	-1246	-176	-1041	(1 + 8 0)
9	-2508	-1244	-193	-1071	(1 + 9 0)
10	-2574	-1244	-192	-1136	(1 + 10 0)
11	-2646	-1243	-193	-1210	(1 + 11 0)
12	-2675	-1242	-194	-1239	(1 + 12 0)
13	-2791	-1242	-194	-1355	(1 + 13 0)
14	-2814	-1240	-194	-1380	(1 + 14 0)

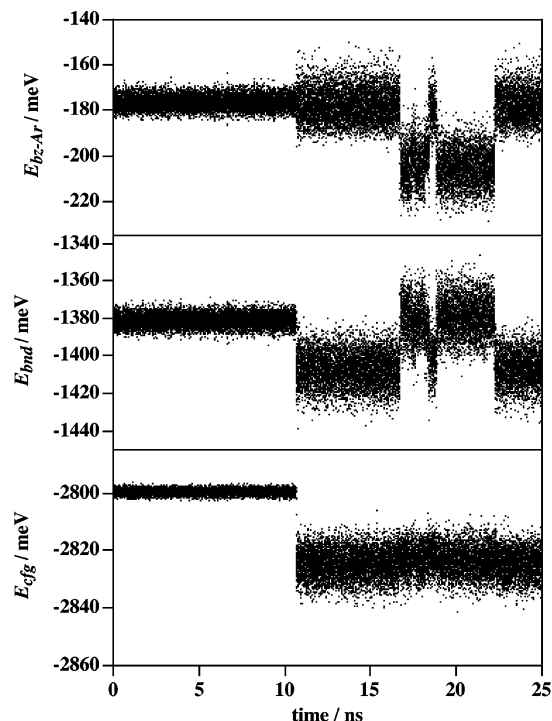
TABLE 2: Energy of the Different Isomers for the $\text{Na}^+ - \text{bz} - \text{Ar}_7$ Clusters

$E_{\text{cfg}}/\text{meV}$	$E_{\text{Na}^+ - \text{bz}}/\text{meV}$	$E_{\text{bz} - \text{Ar}}/\text{meV}$	$E_{\text{bnd}}/\text{meV}$	isomer
-2399	-1246	-155	-998	(1 + 7 0)
-2287	-1248	-212	-827	(1 + 6 1)
-2268	-1248	-210	-810	(1 + 5 2)
-2247	-1248	-219	-780	(1 + 4 3)
-2086	-1249	-216	-625	(1 + 3 4)
-1935	-1249	-213	-473	(1 + 2 5)
-1795	-1249	-209	-337	(1 + 1 6)
-1654	-1249	-204	-201	(1 + 0 7)

wrapping shell is formed around Na^+ . When more Ar atoms are added, these tend to place themselves outside that shell at a much larger distance, leading to a weaker interaction with the benzene molecule. At $n > 14$, when a second shell of Ar atoms is formed around Na^+ , the additional Ar atoms tend to be accommodated near the benzene ring rather than near Na^+ . In this case, clusters with some Ar atoms placed on the benzene surface opposite to the one on which the cation is sitting are more stable than the corresponding $(1 + n|0)$ ones. Accordingly, an increase of the $E_{\text{bz} - \text{Ar}}$ energy contribution has been obtained when increasing the number of Ar atoms from 14 to 19. For instance, for the $\text{Na}^+ - \text{bz} - \text{Ar}_{19}$ cluster, with a configuration energy of -3201 meV, a value of $E_{\text{bz} - \text{Ar}}$ equal to -403 meV was obtained (it must be stressed here that these energy values, due to the mobility of some Ar atoms, cannot be assigned to a particular geometry of the $\text{Na}^+ - \text{bz} - \text{Ar}_{19}$ cluster).

The different contributions to E_{cfg} have been analyzed by considering, for a particular number of Ar atoms (with $n < 14$), the different geometries of the various conformers. Here, the particular case of $n = 7$ has been considered, and related results are shown in Table 2. As can be seen from the table, these clusters become less stable because of an increase of n_2 , and the resulting loss of stability is mainly due to the variation of E_{bnd} . The interaction among two Ar atoms, being lower than that between Na^+ and Ar, leads to a decrease of the attractive interaction as a consequence of the fact that now some Ar atoms negligibly interact with Na^+ .

2.3. Isomeric Transformations. The fact that when the number of solvent Ar atoms increases, some of them end up by occupying less favorable positions and becoming less stable, facilitates the interconversion between different conformers. At low kinetic energy (or low T), a static approach can be taken and isomerization processes can be rationalized in terms of the minimum energy paths connecting potential energy wells. For instance, an inspection of the PES suggests that the isomerization of the $\text{Na}^+ - \text{bz} - \text{Ar}_{14}$ cluster occurs mainly starting from initial configurations in which all the Ar atoms are placed on the same side of the aromatic ring. This is due to the fact that, in order

**Figure 1.** Time evolution of $E_{\text{bz} - \text{Ar}}$ (upper panel), E_{bnd} (central panel) and E_{cfg} (lower panel) for the $\text{Na}^+ - \text{bz} - \text{Ar}_{14}$ cluster (initial configuration $(1 + 14|0)$) calculated at $T = 25$ K.

to displace some Ar atoms to the opposite side of benzene, large variations in some components of E_{cfg} are needed.

Yet, because, strictly speaking, isomeric interconversions between different configurations are dynamical processes, their features are better understood using molecular dynamics means.

For illustrative purposes, the outcomes of a dynamical study of the $\text{Na}^+ - \text{bz} - \text{Ar}_{14}$ performed at $T = 25$ K are shown in Figure 1 by plotting the evolution of some energy contributions as a function of time ($E_{\text{bz} - \text{Ar}}$ in the upper panel, E_{bnd} in the central panel, and E_{cfg} in the bottom panel). The latter shows such a neat sudden switch of the E_{cfg} value at about 10 ns that one is tempted to associate it with an instantaneous change of conformation from the initial to the final isomerization. However, an inspection of the central and upper panel of Figure 1 shows that the process takes place via a more complex mechanism. In fact, the energy contributions plotted in the upper and central panel of Figure 1 ($E_{\text{bz} - \text{Ar}}$ and E_{bnd}) show additional strong interchanges in energy in the time interval going from 17 to 22 ns.

This is better understood by analyzing the evolution in time of the position of the individual atoms. For this purpose, the distances of each Ar atom (i) from the center of mass of benzene ($R(\text{bz} - \text{Ar}_i)$) ($i = 1, \dots, 14$) and from Na^+ ($R(\text{Na}^+ - \text{Ar}_i)$) ($i = 1, \dots, 14$) are plotted in Figures 2 and 3.

The figures show that there are not important changes in the distances during the first 10 ns of the simulation. However, at about 10 ns, sudden variations occur in some $R(\text{bz} - \text{Ar}_i)$ and $R(\text{Na}^+ - \text{Ar}_i)$ distances. Other sudden variations occur in the interval 17–22 ns after a relatively calm interval (10–17 ns). These changes are intimately associated with the isomerization process. As can be seen from the plots of Figures 2 and 3, in fact, the distances from benzene of the atoms initially placed near the cation (see the lowest lying curves) change little during the simulation. The cluster accommodates near Na^+ only five Ar atoms out of the six originally (and finally) placed around it. Four of these six closely placed Ar atoms form a square

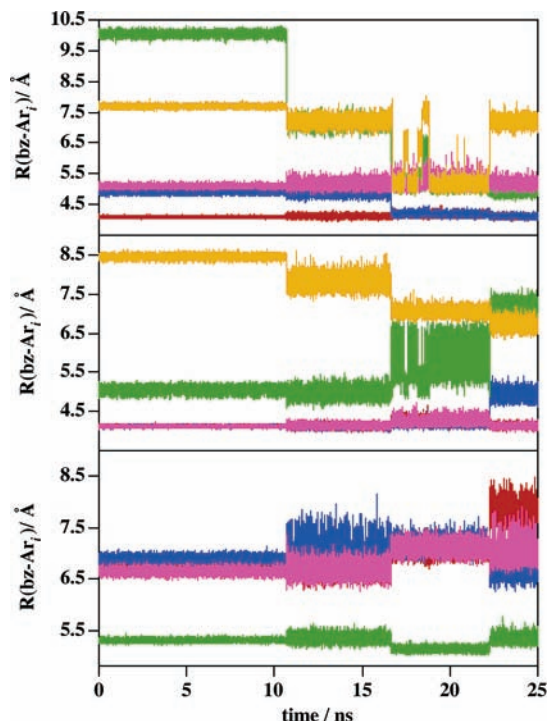


Figure 2. Time evolution of the distances of all Ar atoms from the benzene center of mass for the Na⁺–bz–Ar₁₄ cluster (initial configuration (1 + 14|0)) calculated at $T = 25$ K.

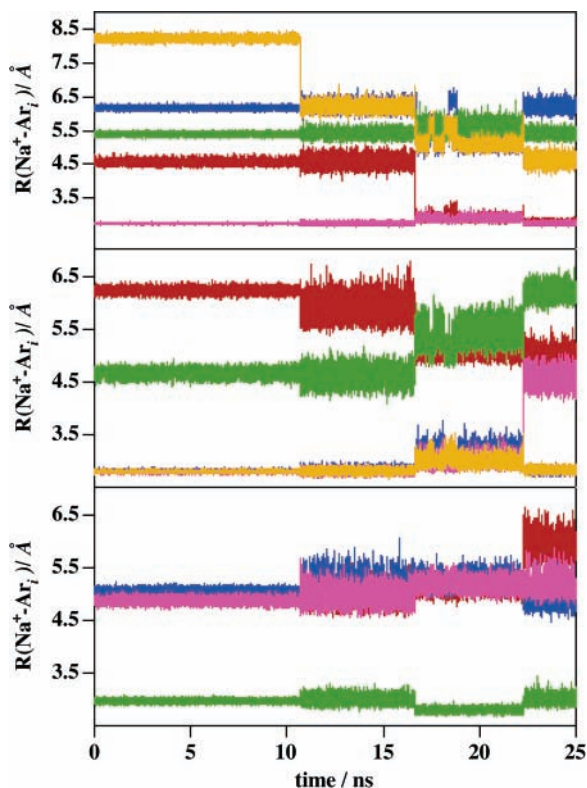


Figure 3. Time evolution of the distances of all Ar atoms from the cation for the Na⁺–bz–Ar₁₄ cluster (initial configuration (1 + 14|0)) calculated at $T = 25$ K.

centered on Na⁺, while a fifth one sits above it to form a quadrangular pyramid encapsulating the cation. The remaining Ar atoms are placed either below or above the plane of the pyramidal basis yet at a large distance. The plots show also that the fifth and the sixth Ar atoms interchange their position during the simulation.

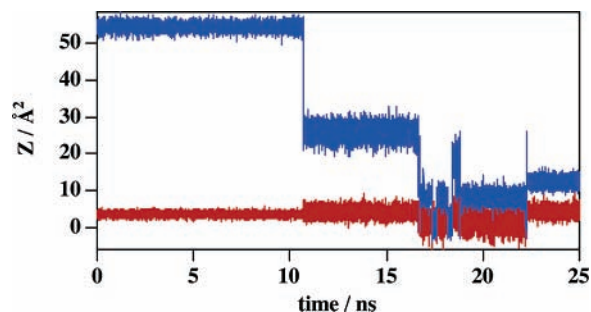


Figure 4. Time evolution of the product (Z) of the distances of Ar and Na⁺ from the benzene plane ($Z > 0$, Ar and Na⁺ are placed on the same side of the benzene plane; $Z < 0$, Ar and Na⁺ are placed on opposite sides of the benzene plane) for the Na⁺–bz–Ar₁₄ cluster (initial configuration (1 + 14|0)) calculated at $T = 25$ K. Red and blue colors represent two different Ar atoms.

To better understand the underlying mechanism, we plotted also the position of the two more mobile Ar atoms with respect to the side of the benzene plane in which the cation is placed (see Figure 4). The figure shows for these two Ar atoms the detail of their flying away to reach the opposite side of the aromatic ring. This is obtained by plotting, for each Ar atom, the product (Z) of its distance from the benzene plane times that of the Na⁺ cation (taken as positive when the atom is on the same side of the Na⁺, negative otherwise) as a function of the simulation time. This means that negative values of the Z indicate that the corresponding Ar atom is placed on the opposite side of the benzene plane with respect to that of the cation. The plot indicates, therefore, that at the beginning, the two Ar preferentially stay by the cation rather than by the benzene molecule. As shown by the blue line of Figure 4, after about 10 ns, one of them starts penetrating the most internal part of the cage (accordingly, the Z value decreases). The other Ar atom (red line in Figure 4), instead, remains close to the benzene plane stabilized by one of the six equivalent on-plane wells of the PES. The figure indicates also that four different PES minima associated with different isomers are explored during the 25 ns of the simulation and that this long duration of the calculations is needed to have a more complete understanding of the isomerization process.

These variations do also reflect themselves in the value of the kinetic energy (E_{kin}). Before the cluster rearranges, the Ar atoms stay near their equilibrium position and this is reflected in an almost constant value of E_{cfc} . Because of total energy conservation, the value of E_{kin} also changes very little before the isomerization process starts. As the isomerization process starts, E_{cfc} changes dramatically and so also does E_{kin} . Moreover, while the isomerization process takes place, E_{kin} oscillates quite widely due to the opening to exploration of new regions of the PES with different configuration energy. This is clearly illustrated in Figure 5, where the kinetic energy for two different cases (with and without isomerization) is plotted as a function of the simulation time.

3. Solvation Dynamics and Mechanisms

The two most important indications provided so far by the simulation are that a quite large number of Ar atoms needs to be considered to carry out a realistic study of the Na⁺–bz–Ar_{*n*} and that, especially when a second (more external) shell is formed, it is more appropriate to refer to the associated Ar atoms as a solvent rather than as components of a cluster because of their high mobility. For this reason, the remainder of the paper

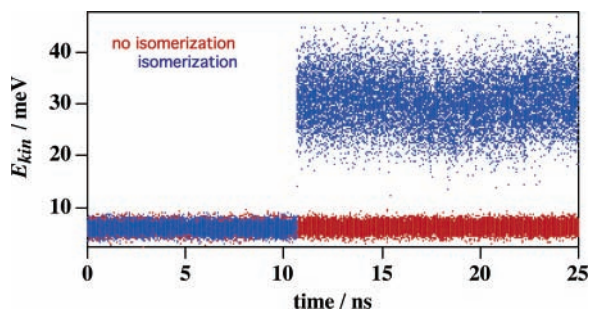


Figure 5. Time evolution of E_{kin} for the $\text{Na}^+ - \text{bz} - \text{Ar}_{14}$ cluster (initial configurations (1 + 14|0), blue line, and (1 + 6|8), red line) calculated at $T = 25$ K.

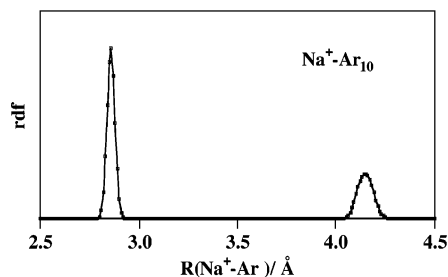


Figure 6. Radial distribution function for the $\text{Na}^+ - \text{Ar}_{10}$ cluster as a function of the distance of Ar atoms from Na^+ .

is devoted to an analysis of solvation processes and analyzes separately the cases of Na^+ , bz, and $\text{Na}^+ - \text{bz}$.

Dynamical calculations have been performed following the same procedure given in Section 2.2. The results have been obtained from simulations long enough (25 ns) to ensure low fluctuations of the energy and temperature mean values and have been analyzed from the radial distribution functions (rdfs) calculated by means of the following equation,

$$\text{rdf} = 4\pi \sum_{i=1}^n r_i^2 P(r_i)$$

where r corresponds either to the distance of Ar atoms from the cation or from the center of mass of benzene.

3.1. The solvation of Na^+ . The dynamics of the solvation of Na^+ has been investigated by surrounding a single Na^+ cation by a variable number, n , of Ar atoms. The results of the simulation show that the Ar atoms tend to place themselves symmetrically around the cation until the first solvation shell is completed. As more Ar atoms are added, their distance from the cation increases. For instance, the radial distribution function (rdf) for $\text{Na}^+ - \text{Ar}_6$ when plotted as a function of the distance of the Ar atoms from Na^+ peaks at 2.71 Å, while the corresponding function for $\text{Na}^+ - \text{Ar}_8$ peaks at 2.85 Å. At $n = 8$, the first solvation shell is completed, and when n further increases, the remaining solvent atoms end up placed in an outer solvation shell. In this case, the radial distribution function shows two peaks, as is the case, for example, of the $\text{Na}^+ - \text{Ar}_{10}$ cluster (see Figure 6). In the figure, the larger peak (associated with eight solvent atoms placed on the first solvation shell) is located at about 2.85 Å, while the smaller peak (associated with the remaining Ar atoms) is located at about 4.15 Å. As the number of solvent atoms further increases, the shape of the Ar atoms distribution around the cation in the second solvation shell reproduces that of the first one.

For these clusters, it has also been observed that some Ar atoms tend to be placed on the same plane in groups of four. This distribution allows the stabilization of the cluster also by

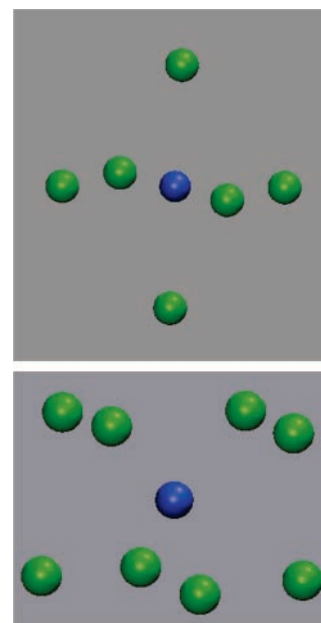


Figure 7. Equilibrium configuration of $\text{Na}^+ - \text{Ar}_6$ (upper panel) and of $\text{Na}^+ - \text{Ar}_8$ (bottom panel).

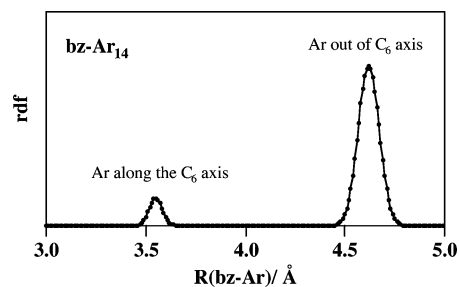


Figure 8. Radial distribution function for the $\text{bz} - \text{Ar}_{14}$ cluster as a function of the distance of Ar atoms from the center of mass of benzene.

the Ar–Ar interactions, for which the minimum of energy is found at a distance of 3.76 Å. As an example, in Figure 7, the equilibrium configuration for $\text{Na}^+ - \text{Ar}_6$ and $\text{Na}^+ - \text{Ar}_8$ clusters are shown. In the equilibrium configuration of $\text{Na}^+ - \text{Ar}_6$, four Ar atoms form a square. The Ar atoms are placed at about 2.7 Å from Na^+ (the $\text{Na}^+ - \text{Ar}$ interaction has the minimum of energy at 2.73 Å). In this configuration, the separation between two Ar atoms is about 3.8 Å. As to the $\text{Na}^+ - \text{Ar}_8$ cluster, its equilibrium configuration is the one for which the Ar atoms are distributed around the cation, being the cluster stabilized by a direct interaction of Ar with Na^+ and with other Ar atoms as well.

3.2. The Solvation of Benzene. The spatial distribution of Ar atoms around the benzene molecule has also been investigated by plotting the rdfs of the Ar atoms with respect to the center of mass of benzene. To discuss in more detail solvation effects, we consider here the $\text{bz} - \text{Ar}_{14}$ cluster because it contains two more rare gas atoms than the 12 corresponding to the symmetric potential energy wells (six above and six below the benzene ring). In Figure 8, the rdf of $\text{bz} - \text{Ar}_{14}$ (isomer (7|7)) is plotted as a function of the distance of the Ar atoms from the center of mass of benzene. The figure clearly indicates that the rdf has two maxima. The first, the smaller one, corresponds to the two Ar atoms placed along the C_6 symmetry axis on both sides of the aromatic ring. The other, the larger one, corresponds to the Ar atoms placed on a plane parallel (either above or below) to the benzene plane. If one bears in mind that, for the $\text{bz} - \text{Ar}$ system, the deepest minimum of the PES is located on

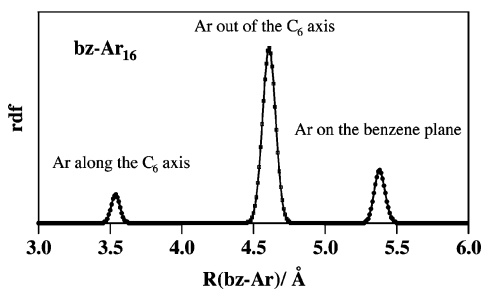


Figure 9. Radial distribution function for the bz–Ar₁₆ cluster as a function of the distance of Ar atoms from the center of mass of benzene.

the symmetry axis at a distance of 3.6 Å from the center of mass of benzene and that the next deepest wells are the six on-plane ones associated with the Ar atom placed at about 5.2 Å (see ref 10), one would not be surprised by the fact that, in our dynamical calculations for the bz–Ar₁₄ system, the radial distribution function peaks at the distances of about 3.5 Å and 4.7 Å.

By increasing the number of Ar atoms, the additional ones preferentially tend to occupy sites near the benzene plane. This is the case, for example, of the bz–Ar₁₆ cluster (isomer (7|2|7)). As shown in Figure 9, in this case, three groups of atoms corresponding to three different distances from the center of mass of benzene are observed. The first two peaks are of the same type as those of Figure 8. On the contrary, the third peak is placed around 5.4 Å, indicating the beginning of formation of another on-plane ring of Ar atoms. This is confirmed also by the plots obtained for the largest cluster considered in our study ($n = 19$).

3.3. The Solvation of Na⁺–Benzene. As expected, the solvation of Na⁺–benzene leads to more complex and highly asymmetric structures than those of Na⁺ and benzene. This fact, together with the different contributions from the various potential energy terms, is responsible for some particular effects occurring mainly when the number of solvent atoms increases. For example, the interaction energy between Na⁺ and Ar at the equilibrium distance is equal to 167 meV, and this value is approximately the same as that of the interaction energy of the bz–Ar₄ cluster. For this reason, when some Ar atoms are unable to reach one of the energetically more favorable positions near the cation, they may end up moving to the opposite side with respect to the benzene plane. When this type of rearrangement occurs, rdf plots become more structured. In this case, it is of some help to consider the solvation shell as formed by two half-shells separated by the aromatic ring.

As already mentioned in Section 2.2, for $n = 1, \dots, 9$, the Ar atoms stay preferentially close to Na⁺. This agrees with the findings of a previous study²⁶ concerned with the K⁺ cation sandwiched by two parallel benzene molecules. In that study, the Ar atoms of the (benzene)₂–K⁺ system solvated by 1, 2, and 3 Ar atoms showed a tendency to intrude the sandwich and to deform it from a parallel to a V-shaped form in order to allow closer interaction between Ar and K⁺. In the single benzene molecule clusters considered here, the benzene remains strongly bound to Na⁺ and the Ar shell is placed around them.

Dynamical calculations show that the first solvation half-shell is saturated when nine Ar atoms are placed near Na⁺. However, it must be taken into account that because of the asymmetry of the cluster, not all Ar atoms are placed at the same distance from the cation. To better illustrate this aspect, we discuss here the Na⁺–bz–Ar₉ and the Na⁺–bz–Ar₁₄ (for $n = 9$, the first solvation semishell reaches completion) systems. Plots of the probability, P_{Ar} , of finding an Ar atom at a certain distance

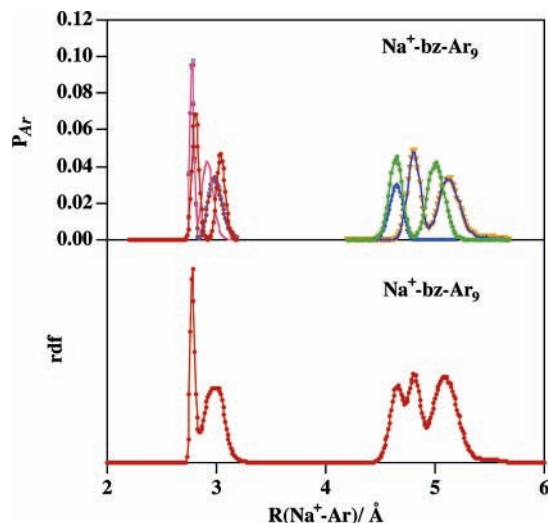


Figure 10. Probability of finding an Ar atom at a certain distance from Na⁺ (upper panel) and radial distribution function (lower panel) for the Na⁺–bz–Ar₉ cluster (initial configuration (1 + 9|0)) as a function of the distance of Ar atoms from Na⁺. The various curves of the upper panel belong to the nine different Ar atoms.

from Na⁺, $R(\text{Na}^+ - \text{Ar})$, and the rdf for the Na⁺–bz–Ar₉ cluster are shown in Figure 10. These results have been obtained by starting the molecular simulations from the (1 + 9|0) isomer. During the simulations, no isomerizations were observed. As apparent from the upper panel of Figure 10, there are two intervals of the Na⁺–Ar distance values for which the probability of finding the Ar atom is high. They are centered around 3 and 5 Å (five of the nine Ar atoms tend to be placed at shorter distance, while the remaining four tend to be placed more far away). This is also shown by the rdf plot given in the lower panel of Figure 10. A similar bimodal rdf is shown also by the Na⁺–Ar₁₀ clusters (see Figure 6), that is, however, less structured than that for Na⁺–bz–Ar₉. This indicates that the presence of benzene in the cluster not only leads to average larger distances for the solvating Ar atoms but also increases their mobility and capacity of interchanging position during the simulation. However, the fact that the two ranges of values are still quite confined implies also that the Ar atoms prefer (at the low-temperature considered) to remain on the same side of the aromatic ring rather than moving on the other side.

By increasing the number of solvent atoms, it has been observed that once the first solvation shell of Na⁺ is completed, the Ar atoms tend to form a second solvation shell (though still closer to Na⁺ than to the benzene molecule as already found for the first shell) and progressively fill it. This second shell is obviously floppier, and when the solvent atoms becomes more numerous, they can more easily interchange their positions.

For Na⁺–bz–Ar₁₄, dynamical simulations have been carried out at $T = 25$ K starting from two different configurations of the solvated cluster. One of them has all of the Ar atoms placed on the same side of the benzene plane with respect to the cation (isomer (1 + 14|0)), while the other has the Ar atoms distributed on both sides of the aromatic ring (isomer (1 + 6|8)).

As shown in the upper panel of Figure 11, the rdf of the Na⁺–bz–Ar₁₄ (1 + 14|0) cluster is much more structured than that of Na⁺–bz–Ar₉. The figure shows, in fact, peaks located at quite large distances. For this cluster, the lowest part of the radial distribution is similar to that of Na⁺–bz–Ar₉. This indicates that some Ar atoms not only are involved in the second solvation shell but also explore larger distances while moving from one side of the benzene plane to the opposite one during

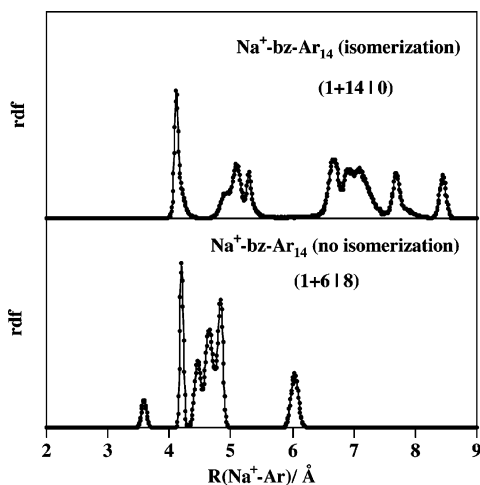


Figure 11. Radial distribution function for the $\text{Na}^+ - \text{bz} - \text{Ar}_{14}$ cluster (initial configurations (1 + 14|0) (upper panel) and (1 + 6|8) (lower panel)) as a function of the distance of Ar atoms from Na^+ .

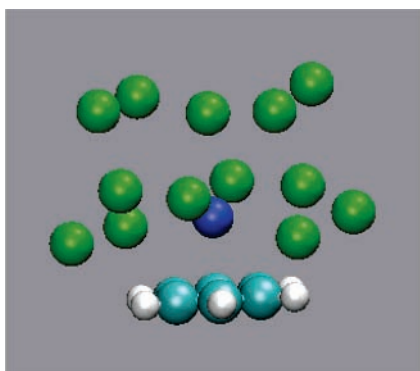


Figure 12. Equilibrium configuration of $\text{Na}^+ - \text{bz} - \text{Ar}_{13}$ cluster (1 + 13|0).

the isomerization process. These results significantly differ from those for the (1 + 6|8) isomer. In this case, as shown by the lower panel of Figure 11, in addition to the expected structure located in the interval ranging from 4 to 5 Å (and due to the fact that the first solvation shell extends over both sides of the aromatic ring), there is a lower peak. This peak corresponds to a configuration having an Ar atom placed along the symmetry axis that occupies the most favorable position on the side of the benzene plane opposite to the cation (absent in isomer (1 + 14|0)). On the contrary, the other peak is located at about 6.0 Å and is associated with an Ar atom placed near the benzene plane. In this case (no isomerization), the displacement of the Ar atoms is minimum during the simulation. All Ar atoms tend, in fact, to be placed on the first sphere of solvation of the $\text{Na}^+ - \text{bz}$ cluster and, consequently, the interaction between the solvent atoms and the ionic cluster is stronger than when some of them are placed in outer solvation spheres.

The tendency of Ar atoms to be distributed in groups of four atoms around Na^+ can be observed also for the $\text{Na}^+ - \text{bz} - \text{Ar}_{13}$ cluster, for which the Ar atoms are placed on three parallel planes. Two planes (those close to the cation) contain only four Ar atoms, while the third one contains one Ar more placed practically at the center of the four atoms and directly interacting with Na^+ . These results can be observed in Figure 12.

4. Conclusions

The detailed study of the composition of the force field of $\text{Na}^+ - \text{bz} - \text{Ar}_n$ clusters has been carried out for systems contain-

ing up to a maximum of 19 rare gas atoms. The study has been conducted by formulating the interaction in terms of atom–bond model potentials and by investigating both the formation of wells on the related PES and the possibility for the system to isomerize. The molecular dynamics investigation of the formation of isomers for different values of n has pointed out some typical features of the arrangement of the rare gas atoms around the $\text{Na}^+ - \text{benzene}$ heterocluster. In particular, it has evidenced the existence of different microenvironments associated with the structure of the minima occurring on the potential energy surface. By carrying out dynamical calculations and analyzing the internuclear distance evolution, these features have been related to the various contributions to the interaction and symmetry. This has contributed to the understanding of the gradual evolution of isomerization processes into solvation mechanisms. Solvation mechanisms were found to significantly depend on the number of added Ar atoms and to be driven by the formation of concentric shells. These shells were found to be symmetric in the case of the bare cation and strongly asymmetric in the case of $\text{Na}^+ - \text{bz}$. Of particular interest for clusters containing benzene was the singling out of two classes of configurations depending on whether the Ar atoms are placed only on one side of the aromatic ring or on both sides.

Acknowledgment. M. Albertí, A. Aguilar, and J. M. Lucas acknowledge financial support from the Spanish DGICYT (project CTQ2004-01102), MEC (project UNBA05-33-001), DURSI (project 2005 PEIR 0051/69), and from the Generalitat de Catalunya (CUR 2001SGR-00041). Also thanks are due to the Centre de Supercomputació de Catalunya CESCA-C⁴ and Fundació Catalana per a la Recerca. A. Laganà and F. Pirani acknowledge financial support from the Italian Ministry of University and Research (MIUR, PRIN 2005 contract nos. 2004033958 and 2005033911_001)

References and Notes

- (1) Douin, S.; Parneix, P.; Amar, F. G.; Bréchnignac, Ph. *J. Phys. Chem. A* **1997**, *101*, 122.
- (2) Leutwyler, S.; Bösiger, J. *Chem. Rev.* **1990**, *90*, 489.
- (3) Leutwyler, S.; Jortner, J. *J. Phys. Chem.* **1987**, *91*, 5558.
- (4) Heidenreich, A.; Bahatt, D.; Ben-Horin, N.; Even, U.; Jortner, J. *J. Chem. Phys.* **1994**, *100*, 6300.
- (5) Schmidt, M.; Le Calvè, J.; Mons, M. *J. Chem. Phys.* **1993**, *98*, 6102 and references therein.
- (6) Castleman, A. W., Jr.; Bowen, K. H., Jr. *J. Phys. Chem.* **1996**, *100*, 12911.
- (7) Cabarcos, O. M.; Weinheimer, J. C.; Lisy, J. M. *J. Chem. Phys.* **1998**, *108*, 5151.
- (8) Cabarcos, O. M.; Weinheimer, J. C.; Lisy, J. M. *J. Chem. Phys.* **1999**, *110*, 8429.
- (9) Morais-Cabral, J. H.; Zhou, Y.; MacKinnon, R. *Nature* **2001**, *414*, 37.
- (10) Pirani, F.; Albertí, M.; Castro, A.; Moix, M.; Cappelletti, D. *Chem. Phys. Lett.* **2004**, *394*, 37.
- (11) Albertí, M.; Castro, A.; Laganà, A.; Pirani, F.; Porrini, M.; Cappelletti, D. *Chem. Phys. Lett.* **2004**, *392*, 514.
- (12) Albertí, M.; Castro, A.; Laganà, A.; Moix, M.; Pirani, F.; Cappelletti, D. *J. Phys. Chem. A* **2005**, *109*, 2906.
- (13) Albertí, M.; Castro, A.; Laganà, A.; Moix, M.; Pirani, F.; Cappelletti, D. *Eur. Phys. J. C* **2006**, *38*, 185.
- (14) Albertí, M.; Aguilar, A.; Lucas, J. M.; Pirani, F.; Cappelletti, D.; Coletti, C.; Re, N. *J. Phys. Chem. A* **2006**, *110*, 9002.
- (15) Albertí, M.; Aguilar, A.; Lucas, J. M.; Cappelletti, D.; Laganà, A.; Pirani, F. *Chem. Phys.* **2006**, *328*, 221.
- (16) Dullweber, A.; Hodges, M. P.; Wales, D. J. *J. Chem. Phys.* **1997**, *106*, 1530.
- (17) Ondrechen, J. M.; Berkovitch-Yellin, Z.; Jortner, J. *J. Am. Chem. Soc.* **1981**, *103*, 6586.
- (18) Mons, M.; Courty, A.; Le Calvè, J.; Piuze, F.; Dimicoli, I. *J. Chem. Phys.* **1997**, *106*, 1676.
- (19) Easter, D. C.; Bailey, L.; Mellot, J.; Tirres, M.; Weiss, T. *J. Chem. Phys.* **1998**, *108*, 6135.

(20) Hartke, B.; Charvat, A.; Reich, M.; Abel, B. *J. Chem. Phys.* **2002**, *116*, 3588.

(21) Giju, K. T.; Roszak, S.; Gora, R. W.; Leszczynski, J. *Chem. Phys. Lett.* **2004**, *391*, 112.

(22) Cambi, R.; Cappelletti, D.; Liuti, G.; Pirani, F. *J. Chem. Phys.* **1991**, *95*, 1852.

(23) Cappelletti, D.; Liuti, G.; Pirani, F. *Chem. Phys. Lett.* **1991**, *183*, 297.

(24) Dougherty, D. A. *Science* **1996**, *271*, 163.

(25) http://www.dl.ac.uk/TCSC/Software/DL_POLY.

(26) Aguilar, A.; Albertí, M.; Laganà, A.; Pacifici, L. *Chem. Phys.* **2006**, *327*, 105.